RESEARCH REPORTS
Biological

D.M. Lyaruu[1], J.F. Medina[2], S. Sarvide[2], T.J.M. Bervoets[1], V. Everts[1], P. DenBesten[3], C.E. Smith[4], and A.L.J.J. Bronckers[1]*

[1]Department of Oral Cell Biology, Academic Centre for Dentistry Amsterdam, University of Amsterdam, and MOVE Research Institute, VU University Amsterdam, Amsterdam, Netherlands; [2]Division of Gene Therapy and Hepatology, School of Medicine/CIMA, University of Navarra, and Ciberehd, Pamplona, Spain; [3]Department of Oral Sciences, University of California, San Francisco, CA, USA; and [4]Facility for Electron Microscopy Research, Department of Anatomy and Cell Biology and Faculty of Dentistry, McGill University, Montreal, Canada; *corresponding author, a.bronckers@acta.nl

J Dent Res 93(1):96-102, 2014

Barrier Formation: Potential Molecular Mechanism of Enamel Fluorosis

ABSTRACT

Enamel fluorosis is an irreversible structural enamel defect following exposure to supraoptimal levels of fluoride during amelogenesis. We hypothesized that fluorosis is associated with excess release of protons during formation of hypermineralized lines in the mineralizing enamel matrix. We tested this concept by analyzing fluorotic enamel defects in wild-type mice and mice deficient in anion exchanger-2a,b (*Ae2a,b*), a transmembrane protein in maturation ameloblasts that exchanges extracellular Cl^- for bicarbonate. Defects were more pronounced in fluorotic *Ae2a,b*$^{-/-}$ mice than in fluorotic heterozygous or wild-type mice. Phenotypes included a hypermineralized surface, extensive subsurface hypomineralization, and multiple hypermineralized lines in deeper enamel. Mineral content decreased in all fluoride-exposed and *Ae2a,b*$^{-/-}$ mice and was strongly correlated with Cl^-. Exposure of enamel surfaces underlying maturation-stage ameloblasts to pH indicator dyes suggested the presence of diffusion barriers in fluorotic enamel. These results support the concept that fluoride stimulates hypermineralization at the mineralization front. This causes increased release of protons, which ameloblasts respond to by secreting more bicarbonates at the expense of Cl^- levels in enamel. The fluoride-induced hypermineralized lines may form barriers that impede diffusion of proteins and mineral ions into the subsurface layers, thereby delaying biomineralization and causing retention of enamel matrix proteins.

KEY WORDS: pH regulation, Slc4a2, chloride, quantitative X-ray microanalysis, hypermineralization, hypomineralization.

DOI: 10.1177/0022034513510944

Received February 25, 2013; Last revision October 3, 2013; Accepted October 4, 2013

A supplemental appendix to this article is published electronically only at http://jdr.sagepub.com/supplemental.

INTRODUCTION

Enamel fluorosis is a developmental disturbance caused by intake of supra-optimal levels of fluoride (F^-) during early childhood (Whitford, 1996; Aoba and Fejerskov, 2002; DenBesten and Li, 2011). The enamel defects consist of horizontal thin white lines, opacities (subsurface porosities), discolorations, and pits of various sizes. The molecular mechanism underlying enamel fluorosis is still unknown.

Enamel formation by ameloblasts is a 2-step event. First, secretory ameloblasts synthesize and secrete a matrix rich in amelogenins, in which long thin crystal ribbons are formed (Smith, 1998). In the maturation stage, most of the matrix is removed and the crystals expand. Maturation ameloblasts have ion-transporting, resorptive, and degrading functions and cyclically transform into 1 of 2 morphologically distinct cell types: ruffle-ended or smooth-ended ameloblasts. The pH of enamel below these cells changes from slightly acidic to neutral (Sasaki *et al.*, 1991; Smith *et al.*, 1996). For unknown reasons, the maturation stage is sensitive to F^- (DenBesten *et al.*, 1985; Richards *et al.*, 1986, Smith *et al.*, 1993).

The first enamel minerals consist of a calcium-poor, apatite-like acidic calcium phosphate salt (octacalcium phosphate, molar Ca/P = 1.33; Brown *et al.*, 1987; LeGeros *et al.*, 1996; Aoba, 1997) or, as more recently described, poorly crystalline amorphous calcium phosphate (molar Ca/P ratio = 1.55; Beniash *et al.*, 2009). These initially formed minerals are less stable, contain carbonate, and are more readily soluble in acids (LeGeros *et al.*, 1996) as compared to more mature hydroxyapatite crystals (molar Ca/P = 1.67). Formation of apatite crystals from calcium and phosphate ions releases large quantities of protons in the enamel space. Various groups have hypothesized that maturation ameloblasts secrete bicarbonate to neutralize the protons released during mineral formation (Smith, 1998; Lacruz *et al.*, 2010a; Simmer *et al.*, 2010; Bronckers *et al.*, 2011).

F^- accelerates crystal formation in solutions (Brown *et al.*, 1987) and induces hypermineralized lines in secretory enamel *in vivo* and *in vitro* (Bronckers *et al.*, 2009). Given the importance of pH regulation by ameloblasts, we hypothesized that in the presence of increasing levels of fluoride, enamel crystals form more rapidly to result in hypermineralized lines. The resulting increased acidification could contribute to the formation of

fluorosed enamel. We addressed this hypothesis by analyzing fluorotic enamel by pH indicators and examining fluorotic defects in a mouse model with dysfunctional anion exchanger 2a,b (solute carrier 4a2/Slc4a2/Ae2a,b). This transmembrane protein is located in the basolateral membranes of maturation ameloblasts and exchanges Cl^- for bicarbonate as a critical step in pH regulation. Disruption of *Ae2a,b* results in formation of hypomineralized enamel (Lyaruu *et al.*, 2008).

MATERIALS & METHODS

Microcomputer Tomography

Eight 20-day-old *Ae2a,b*$^{-/-}$ and 5 wild-type and 5 heterozygous littermate controls were divided into 2 groups and given either 0 or 100 mg of F/L (given as NaCl) for 6 wks. These knockout mice were made on an FVB background, characterized as F^- resistant (Everett *et al.*, 2002). Though prenatal and perinatal lethality of homozygous *Ae2a,b*$^{-/-}$ is high, mice that pass weaning survive well without gross abnormalities (Medina *et al.*, 2003). Hemimandibles were excised, snap-frozen in liquid nitrogen, freeze-dried, embedded in methylmethacrylate, and scanned at a resolution of 8-µm voxels using a µCT-40 high-resolution scanner (Scanco Medical, AG, Bassersdorf, Switzerland) (Bronckers *et al.*, 2013). The shape of the surrounding bone and the position of the molar roots were used as landmarks to obtain the same stages of development for different animals.

Electron Probe Microanalysis

Back-scatter electron detector microscopy and quantitative elemental analysis of enamel were carried out in cross sections of the methylmethacrylate-embedded mouse incisors by electron probe microanalysis at the midsecretory stage and early and late maturation stages with a Jeol Super Probe (JXA-8800) (Lyaruu *et al.*, 2008).

Histology

Maxillae from the *Ae2a,b*$^{-/-}$ and wild-type littermates were fixed by immersion in 5% paraformaldehyde in 0.1M phosphate, decalcified in neutral EDTA, and processed into paraffin sections. Sections were stained with hematoxylin and eosin.

Staining Incisor Enamel From Rat Incisors With pH Indicator Solution

Female Wistar rats (n = 8), 21 days old, were given either 0- or 100-ppm F in drinking water for 6 weeks. After sacrifice blood plasma was collected from the trunk, the mandibles were rapidly dissected free, snap-frozen, and freeze-dried. The bone caps overlying the incisors and enamel organ soft tissues were removed by microdissection to expose the labial surface of the incisor. The incisors were submersed for 3 seconds to 10 minutes in 5 mL of Universal pH indicator (Acros Organics, Fisher, NJ, USA), methyl red solution (1 mg/mL, dissolved either in neutral solution [1µM NaOH, final pH 7.7] or alkaline solution [10mM NaOH, pH 13.2). The teeth were blotted and covered with inverted glass beaker with wetted filter paper to prevent drying out, and photomicrographs were made at 2-minute intervals. Plasma F content determined by a fluoride ion–selective electrode (Radiometer Analytical, type E41M017). All procedures were approved by the Committee for Animal Health and Animal Care of the Vrije Universiteit and the University of Navarra (Spain).

Calculations and Statistics

Comparison of fluorotic *Ae2a,b*$^{+/-}$ heterozygous with fluorotic homozygous wild-type enamel did not show obvious differences in enamel structure (Figures 1a-1c, 2a-2b), or composition (Appendix Table 1). Hence, data from fluorotic wild-type and fluorotic heterozygous *Ae2a,b* mice were pooled and are referred to as *fluorotic wild type*. Differences among all 4 groups were tested by 1-way analysis of variance, linear regression analysis, or unpaired *t* test using Graphpad Instat 3 software ($p < .05$).

RESULTS

Fluorotic Defects Are More Severe in *Ae2a,b*$^{-/-}$ Mice Than Wild-Type Mice

The surface enamel of wild-type mouse incisors had a typical orange stain. This staining was reduced in fluorotic wild-type mice (Appendix Figure 1) and was entirely absent from fluorotic and nonfluorotic *Ae2a,b*$^{-/-}$ mouse incisors, which were chalk white.

Histology showed that late secretory transitional ameloblasts of *Ae2a,b*$^{-/-}$ fluoride-treated mice locally detached from the enamel surface and formed cysts and lines in the enamel matrix (Appendix Figure 2a, 2c, 2d), typically seen after injection of single high doses of fluoride *in vivo*. These changes were not seen in histologic sections of fluorotic or nonfluorotic wild types (Appendix Figure 2b).

Back-scatter electron detector microscopy revealed that maturation-stage enamel of fluoride-treated homozygous wild-type and heterozygous *Ae2a,b* mice was hypomineralized as compared to control wild-type mice (Figure 1a-1c), with a thin hypermineralized surface and an occasional hypermineralized line in deeper enamel. Fluorotic *Ae2a,b* heterozygous enamel was hypomineralized to an equal extent as fluorotic homozygous wild types. Incisors of *Ae2a,b*$^{-/-}$ mice were shorter; the enamel was thinner. The mineral density of maturation stage enamel of fluorotic wild-type mice was reduced by 22% compared to nonfluorotic wild-type values, but had increased by 17% in fluorotic *Ae2a,b*$^{-/-}$ compared to nonfluorotic *Ae2a,b*$^{-/-}$ mice (Figure 2a).

In enamel of fluoride-treated *Ae2a,b*$^{-/-}$ mice, the mineralization defects were dramatically more intense than in fluoride-treated wild-type mice (Figure 1e-1k). At late maturation, the surface was highly hypermineralized, while the subsurface was extensively hypomineralized (Figure 1h-1k). The enamel of fluoride-treated *Ae2a,b*$^{-/-}$ mice contained hypermineralized lines throughout the enamel thickness, that were much more pronounced than in fluoride-treated wild-type enamel. The outer third of the enamel layer was more densely mineralized, but the remaining inner enamel less (Figure 1g). Part of the outer enamel was lost after eruption (Figure 1i, 1k).

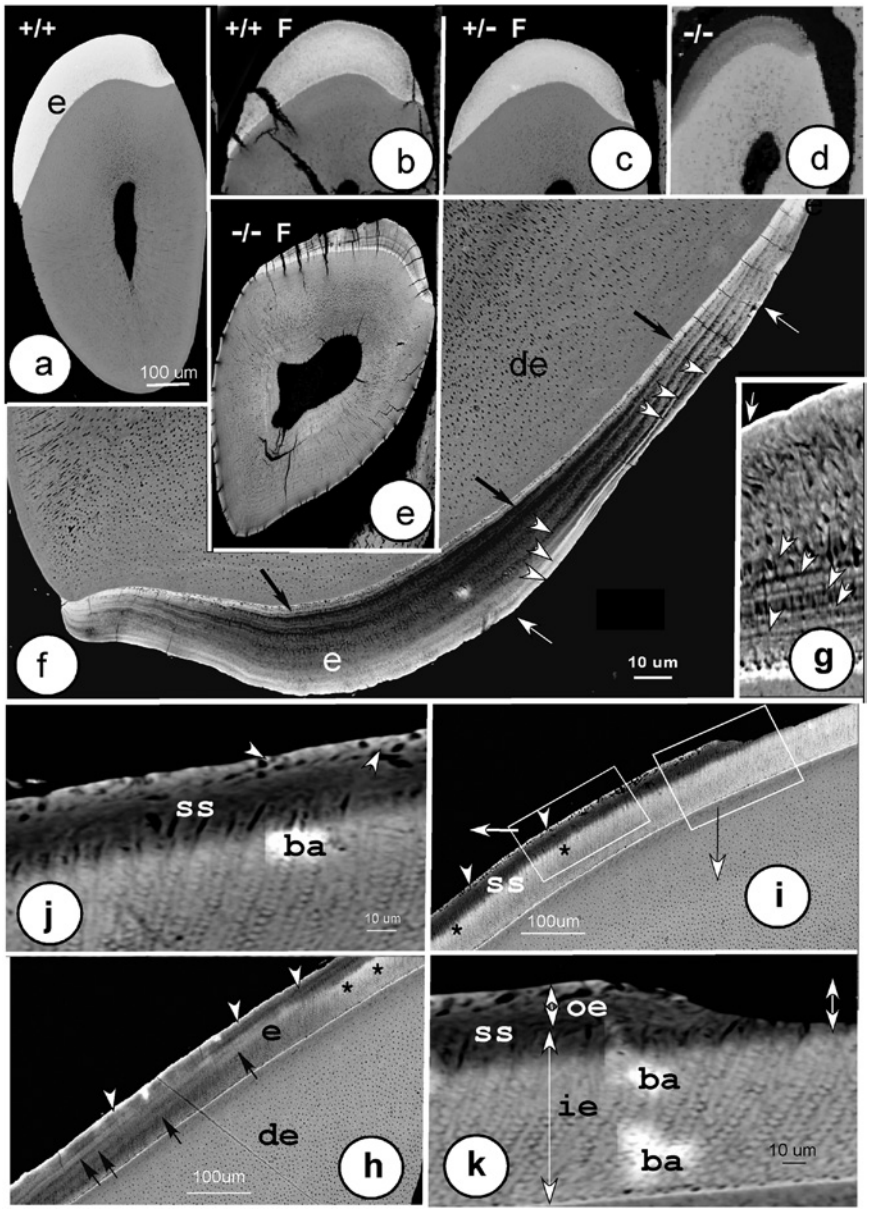

Figure 1. Backscatter images of defects developing in fluorotic maturation-stage enamel in lower incisors. (**a**) Sound homozygous (+/+) wild-type incisor. (**b**) Fluorotic homozygous (+/+) wild-type incisor. (**c**) Fluorotic heterozygous (+/-) *Ae2a,b*$^{+/-}$ mutants. (**d**) Homozygous (-/-) *Ae2a,b*$^{-/-}$ mutant. (**e**) Fluorotic homozygous (-/-) *Ae2a,b*$^{-/-}$ mutant. (e-k) In fluorotic *Ae2a,b*$^{-/-}$ mice, multiple highly mineralized lines (**f, g**; white arrowheads) ran parallel to the surface, often separated by less mineralized bands (f). Surface layers (f, g; white arrows) and dentin-enamel junction (f; black arrows) were strongly mineralized. (**h, i**) Two adjacent areas of enamel in late maturation (left) through eruption (right, sagittal section). The surface layer was extremely hypermineralized (h, i; white arrowheads) throughout the enamel with prominent hypermineralized lines (black arrows). A hypomineralized subsurface zone (ss) lost increasingly more mineral incisally (h-j) and expanded inward into the prismatic inner enamel (i). At the boundary of the subsurface with the inner enamel layer, a more calcified zone formed (h, i; black asterisks). The boxed areas (i) are magnified (**j, k**). The extremely mineralized intact surface was undermined by a hypomineralized subsurface (ss; i, k), and both were lost after eruption (k; double-headed arrow). ba, beam artifacts; e, enamel; de, dentin; p, pulp; ie, inner enamel; oe, outer enamel.

The composition of the enamel as measured by electron probe microanalysis showed differences among the various groups, principally at maturation stage (Table, Appendix Table 2). In enamel of fluoride-treated wild-type mice, the Ca and P content was slightly lower (11%) at the maturation stage and F^- and Ca/P ratio higher (suggesting more mature crystals), although these values did not reach statistical significance, most likely because of the low numbers of mice. S content (a measure for methionine-rich amelogenins) tended to be higher in fluorotic wild-type enamel, suggesting matrix retention.

In enamel of fluoride-treated *Ae2a,b*$^{-/-}$ mice, mineral density (Figure 2a) and Ca and P levels (Table) were substantially lower than in wild-type mice but slightly higher than enamel of *Ae2a,b*$^{-/-}$ mice. The enamel contained 3-fold more F than fluorotic wild-type mice (Table) without clear differences in plasma fluoride levels (10 ± 3.1μM in fluorotic *Ae2a,b*$^{-/-}$ and 10 ± 2.0μM in fluorotic wild-type enamel).

Cl^- Was Decreased in Enamel of Fluorotic Wild-Type and *Ae2a,b*$^{-/-}$ Mice

To determine buffering activity of the ameloblasts in fluoride-treated mice, we tested whether Cl^- levels in enamel could be used as a measure for bicarbonate-Cl^- exchange. Cl^- levels in enamel of wild-type mice increased with ongoing enamel development (Table) and were strongly correlated (r = 0.99) with Ca (Fig 2b). However, exposure to fluoride or disruption of *Ae2a,b* (presumed to lower basolateral influx of Cl^- by ameloblasts) lowered Cl^- in enamel, but Cl^- remained strongly correlated with Ca (r = 0.98 and r = 0.72, respectively; Table, Figure 2b). The correlation curves between Cl^- and Ca in enamel of fluoride-treated wild-type mice had the same slope as wild-type controls, but the curve had shifted downward to lower Cl^- values. This suggested that treatment with fluoride induced a loss of Cl^- relative to calcium—or, expressed in terms of mineralization, a relative increase in Ca

(hypermineralization) reduced the level of Cl^-. Disruption of *Ae2a,b* decreased Cl^- significantly more than treatment with fluoride, creating a much smaller slope value than in wild-type mice, the lowest value in fluoride-treated *Ae2a,b*$^{-/-}$ mice (Table, Figure 2b).

The ratio between Cl^- and Ca was high in enamel of wild-type mice, increased from the secretory to maturation stage, but was significantly lower in enamel of unexposed and fluoride-exposed *Ae2a,b*$^{-/-}$ mice (Table). The reduced Cl^- in enamel of fluoride-treated mice is consistent with our hypothesis that more Cl^- will be exchanged for bicarbonate, required to buffer the excess of protons released at the enamel surface during formation of hypermineralized lines.

Fluorotic Enamel May Impair Diffusion of Protons and Mineral Ions

We then tested the hypothesis that the increased formation of protons, as a result of fluoride-mediated hypermineralization, would result in a more acidic enamel surface.

Rat incisor enamel immersed in Universal pH indicator or pH-neutral methyl-red solution revealed a clear acidic band at the late secretory stage–transitional stage and weaker acidic bands separated by neutral stripes at the maturation stage (Figure 3a, 3b). However, in fluorotic enamel, the acidic bands appeared weaker than in sound enamel and turned neutral alkaline (Figure 3b) after several minutes, suggesting the fluorotic enamel was less acidic than controls. Reduction in pigmentation of the incisors and elevated levels of F^- in plasma (7.5 ± 5.0μM *vs.* 1.2 ± 0.2μM in controls; $p = .022$) confirmed that the experimental rats were fluorotic.

The apparently weaker acidic bands in fluorotic enamel could result from the hypermineralized surface acting as a barrier (Fejerskov *et al.*, 1977; Suga *et al.*, 1987), impairing diffusion of the dyes into the enamel. Alternatively, hypermineralized lines in deep fluorotic enamel could impair diffusion of protons to the surface and acidify an alkaline pH indicator solution. To explore this, we immersed the incisors in alkaline methyl-red solution up to 10 minutes to alkalinize the surface and subsurface layers, mimicking buffering by ameloblasts. In fluorotic enamel, the pronounced acidic band at the transitional stage turned neutral after 6 to 8 minutes (Figure 3c-3g), indicating that acidic bands in the enamel were buffered. However, in nonfluorotic enamel, this took over 20 minutes, suggesting that in fluorotic enamel either (1) the alkaline indicator solution could not penetrate the enamel to a level similar to that of the nonfluorotic sound enamel or (2) protons in the subsurface enamel matrix could not freely diffuse to the surface layers.

DISCUSSION

Regulation of pH by ameloblasts is crucial for sustained crystal growth. Plausibly, maturation ameloblasts use apical anion exchangers of the Slc26 A family (*e.g.*, pendrin) to secrete bicarbonate in exchange for Cl^- (Bronckers *et al.*, 2011; Figure 3c). In the present study, we found that the Cl^- level in enamel of wild-type mice was strongly correlated with that of Ca. Reducing the Cl^- levels (in *Ae2a,b*$^{-/-}$ mice) strongly reduced mineral growth. This is consistent with the concept that mineralization

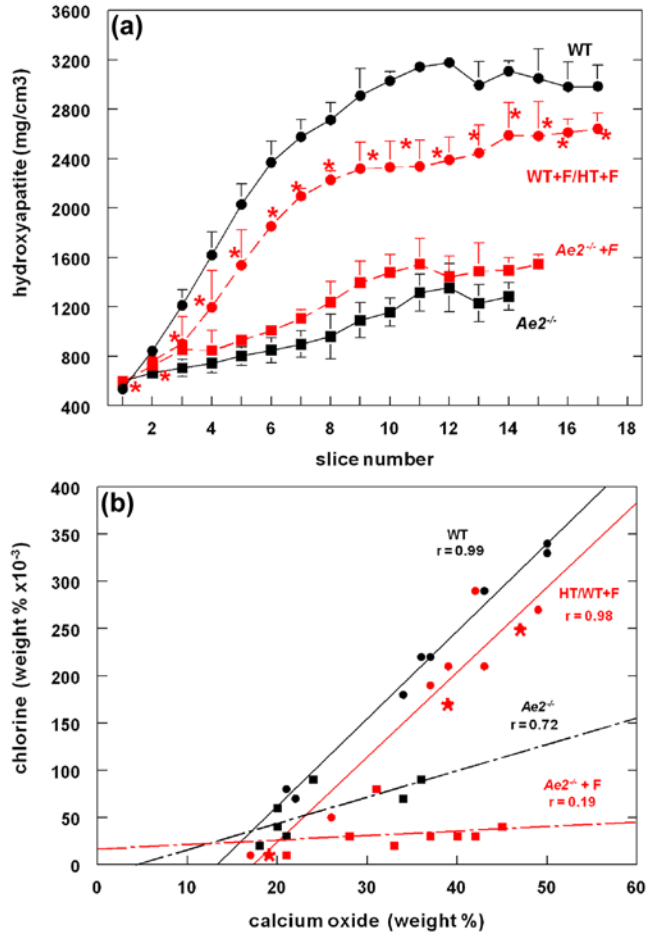

Figure 2. (**a**) Mineral density of mandibular mouse incisor enamel in 4 groups assessed by microcomputer tomography. Wild-type (WT; black circles), fluorotic wild-type, and fluorotic heterozygous (WT+F/HT+F: red circles, n = 3; red asterisk: fluorotic heterozygous, n = 1), *Ae2a,b*$^{-/-}$ (*Ae2*$^{-/-}$: black squares and black drawn line), and fluorotic *Ae2a,b*$^{-/-}$ enamel (*Ae*$^{-/-}$+F: red squares with interrupted red line). In wild-type maturation stage (slices 3-14), fluoride decreases mineralization to 78% ± 3% of nonfluorotic wild-type values ($p < .01$). In *Ae2a,b*$^{-/-}$ enamel, fluoride increased mineralization to 117% ± 8% of unexposed *Ae2a,b*$^{-/-}$ enamel ($p < .01$; *t* test, means and standard deviation; n = 3). (**b**) Correlation between chloride content and calcium in developing mouse incisor enamel, assessed by microprobe analysis. In unexposed wild-type mice (WT; black circles), secretory stage comprises enamel with calcium values between 0% and 22%; early maturation, between 23% and 39%; and late maturation, 40% and higher. Regression curve for WT: y = 9.20x -124, n = 9, r = 0.99, $p < .0001$. Red circles represent values of fluorotic heterozygous mice (HT+F) and red asterisks, fluorotic homozygous wild-type mice (WT+F). For fluorotic WT/HT: y = 9.17x-166, n = 10, r = 0.98, $p < .0001$. For *Ae2a,b*$^{-/-}$ mice (black squares): y = 2.8x -14, n = 7, r = 0.72, $p = .055$. For fluorotic *Ae2a,b*$^{-/-}$ mice (red squares): y = 0.5x -15, n = 8, r = 0.19, $p = .63$. Significance (*p*) value indicates whether the slope is significantly different from zero. r, correlation coefficient (0-1: 0, no correlation; 1, maximal correlation). The shift of Cl^- to a lower level in fluorotic wild-type/heterozygous mice likely reflects a normal rate of secretion of Cl^- (illustrated by the same slope value as in unexposed wild-type mice), followed by loss of Cl^- by an enhanced exchange for intracellular bicarbonate to buffer excess protons released during formation of the hypermineralized line. In *Ae2a,b*$^{-/-}$ mice, the lower Cl^- level is associated with reduced secretion of Cl^-, reflected by the much lower value for the slope than in wild-type mice. In enamel of fluoride-exposed *Ae2a,b*$^{-/-}$ mice, both effects operate.

Table. Composition of Lower Mouse Incisor Enamel from All Groups Determined by Microprobe Analysis, Means ± Standard Deviations

	Composition (% Weight)			
	Ae2a,b$^{-/-}$ Mice (3)*		Fluorotic *Ae2a,b*$^{-/-}$ Mice (5)	
	Secretion (3)**	Late Maturation (3)	Secretion (3)	Late Maturation (5)
CaO	19.97 ± 1.60	35.59 ± 1.76^{a,c}	27.61 ± 6.05	39.80 ± 5.28^{b}
P_2O_5	16.84 ± 1.29	28.93 ± 1.05^{d,f}	23.24 ± 5.89	32.54 ± 4.08^{e}
Molar Ca/P	1.53 ± 0.02	1.59 ± 0.02	1.53 ± 0.08	1.62 ± 0.07
MgO	0.30 ± 0.01	0.51 ± 0.10	0.50 ± 0.25	0.56 ± 0.18^{g,h}
SO_3	0.78 ± 0.02	0.22 ± 0.06	0.70 ± 0.40	0.13 ± 0.19
F	0.02 ± 0.01	0.03 ± 0.01^{k}	0.16 ± 0.11	0.43 ± 0.24^{i,j,k}
Cl	0.03 ± 0.01	0.08 ± 0.01^{m,p,q}	0.02 ± 0.01	0.05 ± 0.03^{n,o,q}
Cl/CaO × 10^{-3}	1.49 ± 0.45^{s}	2.70 ± 0.82^{t,x,y}	0.77 ± 0.28^{u}	1.12 ± 0.78^{w,y,z}
	Wild-type Mice (3)		Fluorotic Wild-type Mice (7)	
	Secretion (3)	Late Maturation (3)	Secretion (3)	Late Maturation (7)
CaO	25.98 ± 7.51	50.16 ± 0.15^{a,b}	21.31 ± 4.26	42.60 ± 4.34^{c}
P_2O_5	21.86 ± 6.41	41.77 ± 0.23^{d,e}	17.41 ± 3.18	34.76 ± 3.22^{f}
Ca/P	1.53 ± 0.01	1.55 ± 0.01	1.56 ± 0.06	1.62 ± 0.05
MgO	0.15 ± 0.01	0.21 ± 0.05^{g}	0.21 ± 0.04	0.22 ± 0.10^{h}
SO_3	0.65 ± 0.36	0.01 ± 0.01	0.95 ± 0.23	0.14 ± 0.19
F	0.04 ± 0.03	0.04 ± 0.01^{i}	0.12 ± 0.06	0.14 ± 0.09^{i}
Cl	0.11 ± 0.06	0.34 ± 0.01^{l,m,n}	0.02 ± 0.02	0.23 ± 0.04^{l,o,p}
Cl/CaO × 10^{-3}	4.05 ± 1.05^{r,s,u}	6.71 ± 0.13^{t,z}	0.92 ± 0.68^{r}	5.31 ± 0.76^{w,x}

Statistical significance was tested for the same developmental stage among different groups. Groups with the same character or symbol are statistically different. For statistics (analysis of variance; see Appendix Table 2): *, number of mice; **, number of developmental stages measured.

depends on the capacity of the ameloblasts to buffer protons by secreting bicarbonates at the expense of Cl^- present in enamel.

We hypothesized that development of fluorosis is associated with transient acidification at the mineralization front, induced by formation of hypermineralized lines. Fluorotic defects were much pronounced in *Ae2a,b*$^{-/-}$ mice in which pH regulation was defective, illustrating that in wild-type mice ameloblasts need Cl^- in enamel fluid to secrete bicarbonate and regulate pH. Lower levels of Cl^- were also found in enamel of fluoride-treated wild-type mice that also developed hypermineralized lines. The reduced amount of Cl^- in fluoride-exposed wild-type mice probably reflects the extra amount of buffer needed to neutralize the acidification resulting from the hypermineralization.

We recently reported that enamel organs of fluorotic mice expressed more transcripts for *Nbce1/Slc4a4* (Zheng *et al.*, 2011) than control mice. Nbce1/Slc4a4 is another potential pH regulator in the enamel organ, which has been shown to respond to acidification (Lacruz *et al.*, 2010b). These studies add further evidence that fluorotic defects are associated with increased acidification.

How these changes eventually result in *hypomineralized* enamel is not yet clear. One possibility is that episodes of acidification (during each intake of fluoridated water) at the mineralization front interrupt mineral transport and delay mineralization. Another possibility is that the hypermineralized lines form a physical barrier that impairs diffusion of ions and peptides (Figure 3b-3g).

Enamel mineralization is unique in that immediately after matrix secretion, long thin crystal ribbons form with a protein matrix filling the intercrystalline spaces. To complete mineralization over the full enamel thickness, these intercrystalline spaces must remain permeable for mineral ions for a considerable period. Hypermineralization lines formed at the secretion stage become less apparent as subsurface mineralization progresses (Figure 3e), while those formed at the maturation stage remain at the surface and gradually intensify (Figure 3f, 3g). Our studies with pH indicator dyes support the possibility that hypermineralized lines may form a physical barrier that impairs ion transport or ion diffusion from surface to deep layers. To further support this possibility, we found that *in vitro* enamel with a fluorotic lesion takes up fewer mineral ions in molar tooth organ cultures (Appendix Figure 3).

This barrier model offers a possible explanation for the reduction in the number of pH cycles and retardation of ameloblast transition from ruffle- to smooth-ended mode in fluorotic teeth

deeper by ongoing deposition of enamel at the surface. Multiple latent thin hyperlines result from episodic F insults after each fluoridated water intake. In the maturation phase at the time of the first F insult, a single hypermineralized line is formed at the surface (f). Subsequent F insults that form the separate lines in the secretion stage will now all concentrate at the maturation-stage surface (g). This intensifies surface hypermineralization. Protons trapped below this barrier recrystallize more-soluble crystals into higher maturity, but crystals cannot expand by lack of mineral ions. A porous subsurface layer develops below a hypermineralized surface.

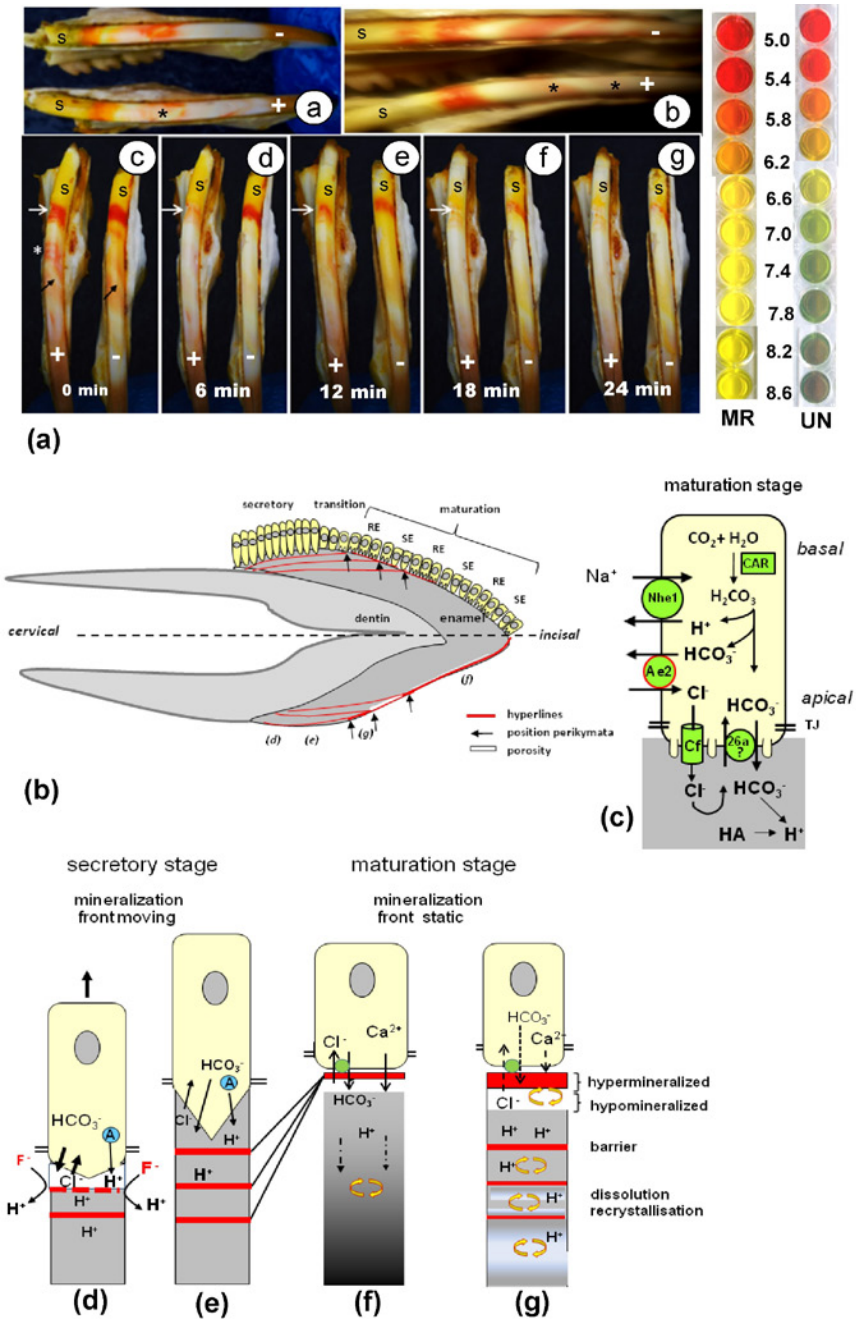

Figure 3. (a) Change in pH in modulation bands in fluorotic rat enamel stained with pH dyes. Fluorotic cell-free rat incisor enamel was stained *ex vivo* with Universal pH indicator (a-a), neutral methyl red; a-b, alkaline methyl red solution [a-c–a-g]. Top right: Colors of methyl red (MR) or Universal indicator (UN) between pH 5.2 and pH 6.8. (a-a, a-b) *Acidic bands (red/pink) in fluorotic (+) incisor stain weakly compared to nonfluorotic (-) control incisor. Secretion stage (s) stains green (neutral) with Universal indicator (a-a) and yellow/white (a-b) with methyl red. In maturation stage, the wide acidic (pink) bands are separated by the narrow neutral (green/white, Universal) or yellow/white (methyl red) stripes (a-c–a-g). Time-lapse micrographs of fluorotic (+) and nonfluorotic (-) developing rat incisor enamel stained with alkaline methyl red for 10 minutes and then photographed every 2 minutes. The most prominent acidic (red) band in fluorotic enamel at the transitional stage (white arrow) is almost gone at 6 minutes but much later in controls (right incisor). Black arrows indicate narrow pH-neutral (yellow-stained) smooth-ended stripes between slightly acidic (pink-stained) ruffle-ended bands. *Several other acidic staining narrow bands that rapidly disappear. (b) Barrier model as molecular mechanism for development of enamel fluorosis. Fluorotic defects projected on a human incisor (characters between parentheses in Fig 3b refer to drawings d-g at the bottom). Arrows point to the transitional stages most sensitive to F where fluorotic lines reach the surface and combine with fluorotic hypermineralized surface. These form the accentuated perikymata. (c) A simplified model of the machinery in maturation ameloblasts to secrete bicarbonate (Bronckers *et al.*, 2011). Cf, cystic fibrosis transmembrane conductance regulator; 26a, anion exchanger of the Slc26a family; Ae2, anion exchanger-2; Car, carbonic anhydrase-2; Nhe1, sodium hydrogen exchanger-1; TJ, tight junction; HA, hydroxyapatite. (d) During the secretory stage, F accelerates crystal growth at the mineralization front below the ameloblasts. This generates an excess of protons that promotes formation of an acid-insoluble F-apatite layer forming a barrier (red). Acidification interrupts mineralization and accelerates bicarbonate secretion at the expense of Cl^-. Amelogenins (A; blue) also buffer. After F clearance, pH is restored and mineralization resumes. (e) The hyperline is buried

(DenBesten *et al.*, 1985; Richards *et al.*, 1986). In these previous studies, ameloblast modulation was measured indirectly by dyes diffused through the open intracellular junctions of smooth-ended ameloblasts, attaching to loosely bound calcium. It is therefore possible that the hypermineralized surface did not allow binding of these dyes. The hypermineralized surface layer could also prevent potential signaling factors in the enamel (protons, ions, or matrix fragments) from reaching ameloblasts to trigger transition from ruffle- to smooth-ended mode. The barrier model does not exclude other potential effects on how fluoride induces enamel defects (DenBesten *et al.*, 2011).

Similar to the fluorotic enamel of *Ae2a,b*$^{-/-}$ mice, teeth of children raised in areas with high levels of fluoride in drinking water have extensive subsurface porosities below an intact well-mineralized surface (Fejerskov *et al.*, 1977; Yanagisawa *et al.*, 1989). Severely fluorotic erupted human enamel contains partly dissolved crystals with central perforations (Yanagisawa *et al.*, 1989), less carbonate, more P, and higher crystallinity (Zavala-Alonso *et al.*, 2012). The development of these surface/subsurface defects may be explained by selective dissolution of crystallites at the maturation stage by protons released during hypermineralization at the surface. These protons could dissolve fluoride-poor immature crystals in the subsurface, particularly in the maturation stage when the ruffle-ended bands are acidic and the mineralization front is stationary, exposing the same surface area repeatedly to fluoride insults (Figure 3f, 3g). The surface itself is well protected by incorporation of F^- into the crystals, increasing their resistance to acid dissolution (Kato *et al.*, 1988).

Collectively, our data support the conclusion that fluoride stimulates enamel hypermineralization, which briefly acidifies enamel matrix. Acidification could influence ion transport and modulation. Hypermineralized bands in the enamel could delay mineralization by acting as a physical barrier, impairing diffusion of ions and peptides.

ACKNOWLEDGMENTS

Part of this work has been presented at the International Conference on Enamel VIII, June 2011, Starved Rock, IL, USA The authors acknowledge Dr. Ronald P. J. Oude Elferink (AMC, University of Amsterdam) and Dr. H. Margolis (Forsythe Center, Boston, MA, USA) for helpful remarks. This work was supported by the National Institutes of Health (grant DE13508). The authors declare no potential conflicts of interest with respect to authorship and/or publication of this article.

REFERENCES

Aoba T (1997). The effect of fluoride on apatite structure and growth. *Crit Rev Oral Biol Med* 8:136-153.

Aoba T, Fejerskov O (2002). Dental fluorosis: chemistry and biology. *Crit Rev Oral Biol Med* 13:155-170.

Beniash E, Metzler RA, Lam RS, Gilbert PU (2009). Transient amorphous calcium phosphate in forming enamel. *J Struct Biol* 166:133-143.

Bronckers AL, Lyaruu DM, DenBesten PK (2009). The impact of fluoride on ameloblasts and the mechanisms of enamel fluorosis. *Crit Rev Oral Biol Med* 88:877-893.

Bronckers AL, Guo J, Zandieh-Doulabi B, Bervoets TJ, Lyaruu DM, Li X, *et al*. (2011). Developmental expression of SLC26A4 (pendrin) during amelogenesis in developing rodent teeth. *Eur J Oral Sci* 119(Suppl 1):185-192.

Bronckers AL, Gueneli N, Lüllmann-Rauch R, Schneppenheim J, Moraru AP, Himmerkus N, *et al*. (2013). The intramembrane protease SPPL2A is critical for tooth enamel formation. *J Bone Miner Res* 28:1622-1630.

Brown WE, Edelman N, Tomzaic BB (1987). Octacalcium phosphate as precursors in biomineral formation. *Adv Dent Res* 1:306-313.

DenBesten P, Li W (2011). Chronic fluoride toxicity: dental fluorosis. *Monogr Oral Sci* 22:81-96.

DenBesten PK, Crenshaw MA, Wilson MH (1985). Changes in the fluoride induced modulation of maturation stage ameloblasts of rats. *J Dent Res* 64:1366-1370.

DenBesten PK, Zhu L, Li W, Tanimoto K, Liu H, Witkowska HE (2011). Fluoride incorporation into apatite crystals delays amelogenin hydrolysis. *Eur J Oral Sci* 119(Suppl 1):3-7.

Everett ET, McHenry MA, Reynolds N, Eggertsson H, Sullivan J, Kantmann C, *et al*. (2002). Dental fluorosis: variability among different inbred mouse strains. *J Dent Res* 81:794-798.

Fejerskov O, Thylstrup A, Larsen J (1977). Clinical and structural features and possible pathogenic mechanisms of dental fluorosis. *Scand J Dent Res* 85:510-534.

Kato K, Nakagaki H, Sakakibara Y, Weatherell JA, Robinson C (1988). The dissolution rate of enamel in acid in developing rat incisors. *Arch Oral Biol* 33:657-660.

Lacruz RS, Nanci A, Kurtz I, Wright JT, Paine ML (2010a). Regulation of pH during amelogenesis. *Calcif Tissue Int* 86:91-103.

Lacruz RS, Nanci A, White SN, Wen X, Wang H, Zalzal SF, *et al*. (2010b). The sodium bicarbonate cotransporter (NBCe1) is essential for normal development of mouse dentition. *J Biol Chem* 285:24432-24438.

LeGeros RZ, Sakae T, Bautista C, Retino M, LeGeros JP (1996). Magnesium and carbonate in enamel and synthetic apatites. *Adv Dent Res* 10:225-231.

Lyaruu DM, Bronckers AL, Mulder L, Mardones P, Medina JF, Kellokumpu S, *et al*. (2008). The anion exchanger *Ae2a,b*$^{-/-}$ mice is required for enamel maturation in mouse teeth. *Matrix Biol* 27:119-127.

Medina JF, Recalde S, Prieto J, Lecanda J, Saez E, Funk CD, *et al*. (2003). Anion exchanger 2 is essential; for spermiogenesis in mice. *Proc Nat Acad Sci U S A* 100:15847-15852.

Richards A, Kragstrup J, Josephsen K, Fejerskov O (1986). Dental fluorosis developed in post secretory enamel. *J Dent Res* 65:1406-1409.

Sasaki S, Takagi T, Suzuki M (1991). Cyclical changes in pH in bovine developing enamel sequential bands. *Arch Oral Biol* 36:227-231.

Simmer JP, Papagerakis P, Smith CE, Fisher DC, Rountrey AN, Zheng L, *et al*. (2010). Regulation of dental enamel shape and hardness. *J Dent Res* 89:1024-1038.

Smith CE (1998). Cellular and chemical events during enamel maturation. *Crit Rev Oral Biol Med* 9:128-161.

Smith CE, Nanci A, Denbesten PK (1993). Effects of chronic fluoride exposure on morphometric parameters defining the stages of amelogenesis and ameloblast modulation in rat incisors. *Anat Rec* 237:243-258.

Smith CE, Issid M, Margolis HC, Moreno EC (1996). Developmental changes in the pH of enamel fluid and its effects on matrix resident proteinases. *Adv Dent Res* 10:159-169.

Suga S, Aoki H, Yamashita Y, Tsuno M, Ogawa M (1987). A comparative study of disturbed mineralization of rat incisor enamel induced by strontium and fluoride administration. *Adv Dent Res* 1:339-355.

Whitford GM (1996). The metabolism and toxicity of fluoride, 2nd revised ed. Basel, Switzerland: Karger.

Yanagisawa T, Takuma S, Tohda H, Fejerskov O, Fearnhead RW (1989). High resolution electron microscopy of enamel crystals in cases of human dental fluorosis. *J Electron Microsc (Tokyo)* 38:441-448.

Zavala-Alonso V, Loyola-Rodríguez JP, Terrones H, Patiño-Marín N, Martínez-Castañón GA, Anusavice K (2012). Analysis of the molecular structure of human enamel with fluorosis using micro-Raman spectroscopy. *J Oral Sci* 54:93-98.

Zheng L, Zhang Y, He P, Kim J, Schneider R, Bronckers AL, *et al*. (2011). NBCe1 in mouse and human ameloblasts may be indirectly regulated by fluoride. *J Dent Res* 90:782-787.